J Appl Electrochem (2009) 39:1871–1876
DOI 10.1007/s10800-009-9891-5

ORIGINAL PAPER

Preparation and properties of Co_3O_4 nanorods as supercapacitor material

Li Cui · Juan Li · Xiao-Gang Zhang

Received: 2 October 2008 / Accepted: 29 March 2009 / Published online: 14 April 2009

Abstract Co_3O_4 nanorods have been successfully synthesized by thermal decomposition of the precursor prepared via a facile and efficient microwave-assisted hydrothermal method, using cetyltrimethylammonium bromide (CTAB) with ordered chain structures as soft template for the first time. The obtained Co_3O_4 was characterized by X-ray diffraction (XRD), scanning electron microscopy (SEM), transmission electron microscopy (TEM), and electrochemical measurements. The results demonstrate that the as-synthesized nanorods are single crystalline with an average diameter of about 20 to 50 nm and length up to several micrometers. Preliminary electrochemical studies, including cyclic voltammetry (CV), galvanostatic charge–discharge, and electrochemical impedance spectroscopy (EIS) measurements, are carried out in 6 M KOH electrolyte. Specific capacitance of 456 F g^{-1} for a single electrode could be achieved even after 500 cycles, suggesting its potential application in electrochemical capacitors. This promising method could provide a universal green chemistry approach to synthesize other low-cost and environmentally friendly transition metal hydroxide or oxide.

L. Cui · J. Li (✉)
College of Chemistry and Chemical Engineering, Xinjiang University, 830046 Urumqi, People's Republic of China
e-mail: lj-panpan@163.com

J. Li
School of Science, Xi'an Jiaotong University, 710049 Xi'an, People's Republic of China

X.-G. Zhang
College of Material Science and Technology, Nanjing University of Aeronautics and Astronautics, 210016 Nanjing, People's Republic of China

Keywords Microwave-assisted hydrothermal synthesis · CTAB template · Co_3O_4 nanorods · Supercapacitor material

1 Introduction

Supercapacitors, also called electrochemical capacitors (ECs), are attracting more and more attention in the field of energy storage device and conversion. Compared with the conventional batteries, ECs have superb characteristics of larger power density and longer cycling life [1]. The supercapacitors are being developed in a variety of applications such as mobile electronic devices, back-up power supplies, and hybrid electric vehicles [2, 3]. In general, the energy storage is either capacitive or pseudocapacitive in nature. The capacitive or non-faradaic process is based on charge separation at the electrode/solution interface, whereas the pseudocapacitive process consists of fast and reversible faradaic redox reactions that can occur within the electroactive materials having several oxidation states. The electrode materials for ECs are carbon, conducting polymers, and transition metal oxides. Among the many metal oxides investigated as electrode materials for pseudocapacitors, hydrous RuO_2 has shown outstanding properties. The amorphous $RuO_2 \times H_2O$ formed by sol–gel method shows a specific capacitance as high as 720 F g^{-1} in acidic electrolyte, which was known as a large breakthrough in supercapacitors [4]. However, despite the superior performance of this material, the high cost and toxic nature limit its large-scale commercialization in electrochemical supercapacitors. Hence, considerable efforts have been devoted to develop alternative or inexpensive electrode materials with good capacitive characteristics, such as NiO [5, 6], CoO_x [7–9], MnO_2 [10, 11], $Ni(OH)_2$ [12], and $Co(OH)_2$ [13] etc.

Among a wide variety of materials, spinel Co_3O_4 has attracted a great amount of attention and becomes one of the most important functional materials due to its unique application in heterogeneous catalysts [14], anode materials in Li-ion rechargeable batteries [15], solid-state sensor [16], solar energy absorbers [17], ceramic pigments, and electrochromic devices [18]. Even if the cycle reversibility is not good, Co_3O_4 is considered as one promising potential candidate for supercapacitors because of its environmental friendliness, low cost, and favorable pseudocapacitive characteristics [8]. In some reports, Co_3O_4 electrode was studied and it exhibited good electrochemical performance in alkaline solutions [19]. These advantages make spinel Co_3O_4 promising as a alternative material of noble metals.

In recent years, one-dimensional (1D) nanostructures, such as nanotubes, nanorods, nanowires, and nanoribbons, have attracted considerable interest for scientific research, because of their remarkable electronic, magnetic, optical, catalytic, and mechanical properties. The 2D or 3D structured materials that are nano- or micro-sized assembled by 1D nano-scale building blocks have also been pursued and are expected to provide novel and unexpected properties. In addition, the electrodes based on nanomaterials have demonstrated better rate capabilities than those of traditional materials. Many modern methods based on physical and chemical approaches have been developed for the synthesis of size and shape dependent one-dimensional materials. Among these, microwave-assisted heating method has attracted considerable attention in the preparation of nanomaterials, due to the advantages of fast reaction rate, short reaction time, high reaction selectivity, and energy saving [20–23]. Although microwave heating has been applied for the synthesis of a variety of nanoparticles, there are few reports on the synthesis of one-dimensional nanomaterials by microwave method, and to the best of our knowledge, most of methods for the synthesis of Co_3O_4 nanomaterials involved the introduction of other elements, high-temperature, and/or more time [15, 24, 25]. Herein, a novel and facile microwave-assisted strategy has been proposed to synthesize rod-like Co_3O_4 as electrode materials for supercapacitors in the presence of CTAB. All the electrochemical tests demonstrate that the prepared material possesses good electrochemical performance.

2 Experimental

The Co_3O_4 nanorods were synthesized under microwave hydrothermal condition. All of the chemical reagents used in the experiment were of analytical grade and were without further purification. In a typical procedure, 0.004 mol $Co(NO_3)_2 \cdot 6H_2O$, 0.016 mol urea, and 1 g CTAB were dissolved in deionized water (100 mL) at room temperature by magnetic stirring. The mixture was stirred vigorously for 10 min until a transparent red solution was formed, and then transferred into a Teflon-lined autoclave specially designed for microwave heating, which was filled up to 80% of the total volume, sealed, and heated for 20 min at a power of 40% of total power (800 W) in a commercial microwave oven (XH-100B, Beijing, PR China). The obtained precipitate was allowed to cool down to room temperature naturally, then collected and washed with distilled water and anhydrous alcohol several times, and then dried at 50 °C under vacuum. The final product, Co_3O_4 nanorods, were obtained by thermal treatment of the above precursors at 200 °C for 3 h in a muffle furnace. The chemical reactions of the above-mentioned synthetic process are supposed as follows:

(1)

$$\text{Hydrothermal reaction: } 2Co(NO_3)_2 + 2CO(NH_2)_2 + 5H_2O \rightarrow Co_2(OH)_2CO_3 \downarrow + 4NH_4NO_3 + CO_2 \uparrow$$

(2)

$$\text{Heat-treatment: } 3Co_2(OH)_2CO_3 + O_2 \rightarrow 2Co_3O_4 + 3H_2O \uparrow + 3CO_2 \uparrow$$

The structure of the product was identified by X-ray diffraction analysis (XRD, Japan Rigaku D/Max 2400) using Cu$K\alpha$ radiation ($\lambda = 1.5405$Å) with a scanning step of 0.02° in the 2θ range of 10 to 80°. The grain size and morphology were observed by transmission electron microscopy (TEM, Model Hitachi H-600, 200 kV) and scanning electron microscopy (SEM, Germany, Leo1430VP).

Electrodes for supercapacitors were prepared by mixing active materials (5 mg) with 25% acetylene black and 5% polytetrafluoroethylene (PTFE) binder. A small amount of water was then added to the above mixture to make a more homogeneous slurry. The slurry was pressed on a nickel mesh under the pressure of 15 MPa, which served as a current collector and the loading density of the electroactive materials was 5 mg cm^{-2}. The prepared electrode was dried at 50 °C for 24 h.

Electrochemical studies were carried out in a three-electrode system, and the freshly prepared rod-like Co_3O_4 on nickel mesh, a platinum electrode, and a Ag/AgCl electrode were used as the working electrode, counter electrode, and reference electrode, respectively. The electrolyte was 6 M KOH solution. Cyclic voltammograms and galvanostatic charge–discharge in a certain potential range were performed using a CHI660A electrochemical working station system (Shanghai) at the room temperature. The electrochemical impedance spectroscopy (EIS) measurements were

performed at open-circuit potential by using an AUTOLAB PGSTAT30. Data were collected in the frequency range of 10^5 to 10^{-2} Hz taking ten points per decade.

3 Results and discussion

In order to investigate the morphology of the as-prepared sample on a large scale, the sample obtained by using CTAB as the soft template was characterized by scanning electron microscopy (SEM). Figure 1a and b displays the low- and high-magnification SEM images of the sample, respectively. The overall morphology of the sample formed by the microwave-assisted hydrothermal synthesis indicates that the product is composed of a great deal of rods with an average diameter of 20 to 50 nm and length up to several micrometers. The sample was relatively uniform when CTAB was introduced into the hydrothermal reaction. Therefore, in this paper, we propose that CTAB, as an important cationic surfactant, has major effect on the growth of Co_3O_4 nanostructures, because their uniform and ordered chain structures can be used conveniently to form rod-like nanostructure materials. The role of this surfactant in the formation of nanorods had been discussed in other literature [26].

Morphology of the obtained Co_3O_4 particles were also examined by TEM images, as shown in Fig. 2. The results confirmed SEM observation that the synthesized nanorods were straight. Since the capacity of the electrode material is significantly influenced by its surface area and morphology, the observed morphology of rods above was a key factor to affect their ultimate electrochemical performances.

The crystalline structure of Co_3O_4 is further characterized using an X-ray diffractometer. As shown in Fig. 3, all peaks ($2\theta = 19.08$, 31.3, 36.8, 44.7, 59.7, 65.3°) shown could be indexed to the spinel Co_3O_4. The broadening of diffraction peaks demonstrates the crystalline character of the nanorod-like Co_3O_4. The result is in good agreement with the standard spectrum (JCPDS, No.42-1467). No peaks of other impurity phases have been detected, indicating that the product is of high purity.

Potential sweep cyclic voltammetric measurements (CV) were performed in a potential range between −0.1 and 0.5 V (versus Ag/AgCl) to examine the electrochemical characteristics and quantify the specific capacitance of the prepared Co_3O_4 electrode. Figure 4 shows the cyclic voltammograms of rod-like Co_3O_4 synthesized by microwave-assisted hydrothermal using CTAB as a template in 6 M KOH electrolyte at the scan rates of 10, 15, and 20 mV s^{-1}. As can be seen in Fig. 4, the Co_3O_4 electrode shows the pseudocapacitance caused by electrochemical reactions. Two pairs of redox reaction peaks (p_1/p_2 and p_3/p_4) are visible in the CV curves, which can be found responsible for the redox process of Co_3O_4. The mechanism of electrochemical reactions of Co_3O_4 in alkaline electrolyte is still not fully understood, but the peak of p_1/p_2 (0.34/0.13 V) may be attributed to the redox transition of Co^{2+}/Co^{3+}, while peak of p_3/p_4 (0.4/0.25 V) may be assigned to the redox transition of Co^{3+}/Co^{4+} [27]. Furthermore, the shape of the CV curves reveals that the capacitive characteristic of Co_3O_4 phase is quite distinct from that of the electric double-layer capacitor, which would produce a CV curve close to an ideal rectangular shape. The peak current also increases with increasing scan rate from 10 to 20 mV s^{-1}.

The electrochemical cyclability of the Co_3O_4 nanorods electrode in 6 M KOH electrolyte was examined by galvanostatic charge–discharge cycles tests at the current of 5 mA, which is equivalent to a current density of 1 A g^{-1}. The specific capacitance can be obtained by $I \times \Delta t / \Delta V \times m$ from the discharge curves, where I is the galvanostatic discharging current (5 mA) and Δt is the discharging time, ΔV is the potential drop during discharge, and m represents the mass of electroactive material (5 mg). According to the equation, the capacitances of Co_3O_4 nanorod material are calculated and listed in Table 1. From the data of Table 1, it is found that the specific capacitance of the electrode based on the as-prepared Co_3O_4 nanorods

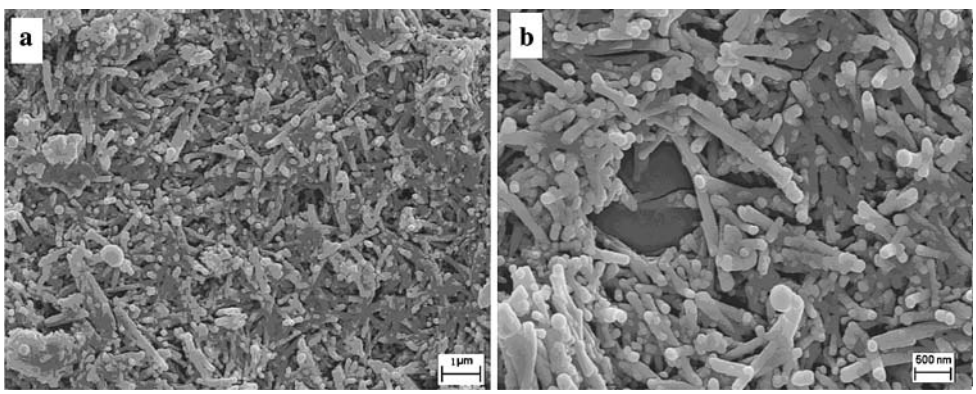

Fig. 1 SEM images of the as-prepared Co_3O_4 nanorods by thermal treatment at 200 °C

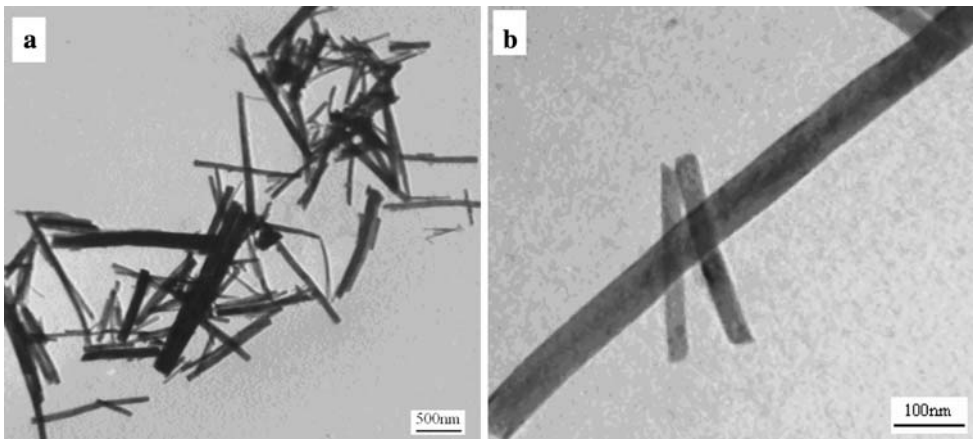

Fig. 2 TEM images of the Co_3O_4 nanorods

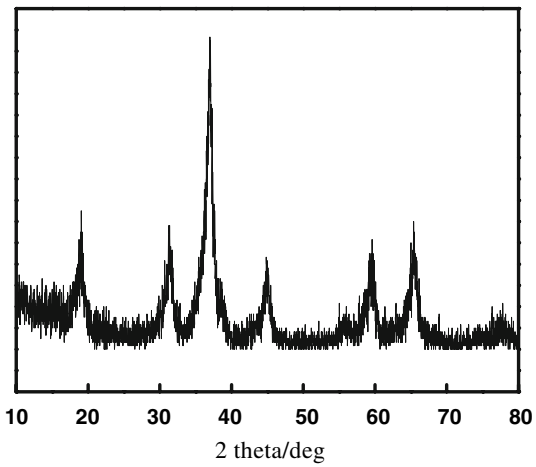

Fig. 3 XRD pattern of the prepared Co_3O_4 nanorods synthesized by microwave-assisted hydrothermal method

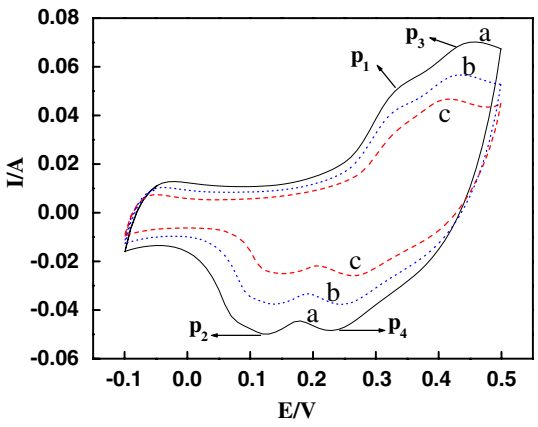

Fig. 4 Cyclic voltammograms (CV) behavior of Co_3O_4 nanorods in 6 M KOH electrolyte at various scan rates of (*a*) 20 mV s^{-1}, (*b*) 15 mV s^{-1}, and (*c*) 10 mV s^{-1}

increases continuously until the 400th cycle, then reached a maximum specific capacitance of 456 F g^{-1} and its capacitance gradually became stable till the 500th cycle. Apparently, the charge–discharge curve is asymmetric in the first cycle and becomes symmetric at 400th cycle. This may be due to that the superficial active sites of the electrode materials have been electrochemically activated in the process of cyclic voltammetry. This indicates that the electrode could endure 500 cycles without significant loss of capacitance and has a potential application as a candidate for ECs.

Table 1 Cycle number versus capacitor of Co_3O_4 nanorod at a current density of 1 A g^{-1}

Cycle number	1	100	200	300	400	500
Capacitance (F g^{-1})	352	375	400	425	456	456

In order to acquire more detail information concerning the capability of Co_3O_4 nanorods, the typical charge–discharge behaviors of the Co_3O_4 electrode at the 1st and 500th cycle are shown in Fig. 5. During the charge and discharge steps, the curves display two variation ranges. A perfect variation of potential versus time dependence (below 0.15 V) parallel to the potential axis would have indicated pure double-layer capacitance behavior from the charge separation at the electrode/electrolyte interface. In contrast, a sloped variation of potential versus time (0.15–0.4 V), caused by electrochemical adsorption/desorption or a redox reaction at the electrode/electrolyte interface, indicates the typical pseudocapacitive property. The specific capacitance of the electrode was 352 and 456 F g^{-1} at the 1st and 500th cycle, respectively, calculated from Fig. 5, which is competitive with the best supercapacitor material, RuO_2 (720 F g^{-1}) for a single electrode [4]. What is more, the cost of Co_3O_4 is remarkably lower than that of RuO_2.

After charging and discharging for 500 cycles at the current density of 1 A g^{-1}, the cyclic voltammetry behavior of the material, as shown in Fig. 6, had been tested again. It can be observed that the electrochemical behavior of the Co_3O_4 electrode is quite different from that of the pre-galvanostatic charge–discharge. The cathodic peak P_4 is hardly changed, while the current of peak

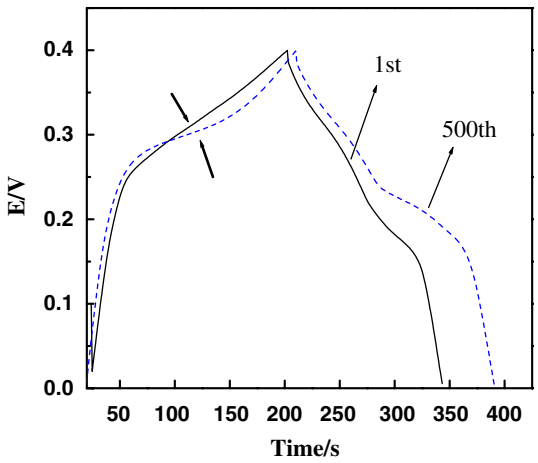

Fig. 5 Galvanostatic charging–discharging curves of Co_3O_4 nanorods at the 1st and 500th cycle measured at the current density of 1A g^{-1}

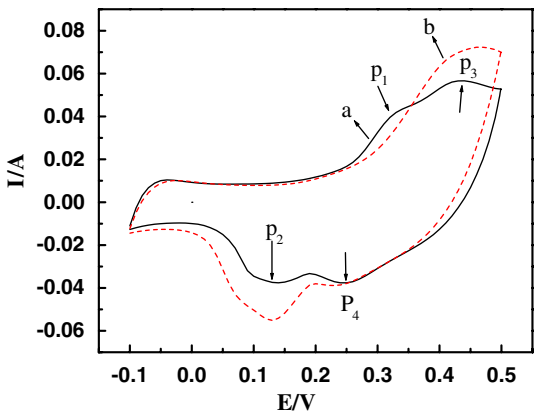

Fig. 6 Cyclic voltammograms of Co_3O_4 nanorods at the scan rate of 15 mV s^{-1}. *a* Pre-galvanostatic charge-discharge. *b* After charging–discharging for 500 cycles at the current density of 1A g^{-1}

P_2 increased apparently, which goes all the way in the discharging curve of Fig. 5. On the other hand, the anodic peaks p_1 and p_3 had merged into one and the peak current value had also apparently increased, which should be consistent with the charging curve of the 500th cycle in Fig. 5 having a notable slope variation (as shown in arrow of Fig. 5 ranging from 0.25 to 0.35 V) of potential versus time dependence parallel to the time axis. Since the degree of electrochemical polarization is greater than that of the galvanostatic charge–discharge process, it also can be seen that the potential of the cathodic peak is more negative than the discharge platform potential, while the anodic peak is converted to a slightly positive direction than the charge platform potential. The peak of the cyclic voltammogram curve, similar to the potential platform of the charge–discharge curve, indicates typical pseudocapacitance behavior, caused by a charge transfer reaction or electrochemical adsorption/desorption process at the electrode/

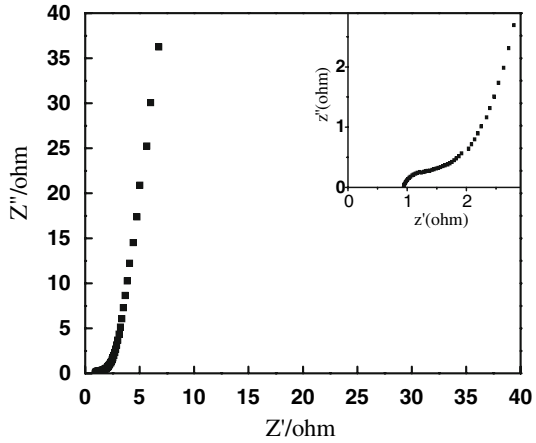

Fig. 7 Impedance plot of Co_3O_4 nanorods electrode

electrolyte interface. The capacitance of Co_3O_4 nanorods mainly result from pseudocapacitive capacitance.

Furthermore, electrochemical impedance spectroscopy was also carried out to prove the capacitive performance at the open-circuit potential in the frequency range of 0.01 to 10^5 Hz with ac-voltage amplitude of 5 mV. The typical Nyquist plot of Co_3O_4 electrode is given in Fig. 7. Judged from the point of intersection of the real axis in the range of the high frequency, the internal resistance of the electrode in an open circuit condition is lower than 1 Ω, which is composed of the following terms: the ionic resistance of electrolyte, the intrinsic resistance of the active material, and the contact resistance at the active material/current collector interface. In the high-to-medium frequency region, one semicircle can be discovered as shown in the up-right corner of Fig. 7, which should be attributed to the charge transfer process at the electrode/electrolyte interface. In low frequency, the impedance plot exhibited a sloppy line of diffusion process in a solid, which is the characteristic feature of pure capacitive behavior. All the above-mentioned results demonstrate that Co_3O_4 nanorods have a really good frequency response and are suitable to be used in electrode material for electrochemical capacitor.

4 Conclusion

A simple and effective microwave-assisted hydrothermal method was proposed to prepare a kind of electrode material of ECs, Co_3O_4, in this study. It is discovered from our experiment that a uniform rod-like Co_3O_4 with perfect crystallinity and regular morphology was formed by using cetyltrimethylammonium bromide (CTAB) as a soft template. Electrochemical measurements indicated that the as-synthesized material could deliver a maximum specific capacitance of 456 F g^{-1} for a single electrode and good

stability over 500 cycles. The high specific capacitance coupled with the low cost and simple preparation method render Co_3O_4 attractive for practical and large-scale applications in a supercapacitor.

Acknowledgements This study has been supported by the National Natural Science Foundation of China (No.20663006). We also thank Scientific Research Program of the Higher Education Institution of Xinjiang (XJEDU2006S206) for partial support of this study.

References

1. Conway BE (1999) Electrochemical supercapacitors. Kluwer Academic/Plenum Publishers, New York
2. Subramanian V, Zhu H, Vajtai R, Ajayan PM, Wei B (2005) J Phys Chem B 109:20207
3. Sarangapani S, Tilak BV, Chen CP (1996) J Electrochem Soc 143: 3791
4. Zheng JP, Jow TR (1995) J Electrochem Soc 142:6
5. Kuo C, Mare AA (1996) J Electrochem Soc 143:124
6. Yuan CZ, Gao B, Su LH, Zhang XG (2008) Solid State Ion 178:1859
7. Cao L, Zhao YK, Lu M, Li HL (2003) J Chin Sci Bull 48:1212
8. Liu Y, Zhao WW, Zhang XG (2008) Electrochim Acta 8:3296
9. Wang Y, Zhang WS, Evans DG, Duan X (2005) J Electrochem Soc 152:A2130
10. Chang JK, Lin CT, Tsai WT (2004) Electrochem Commun 6:666
11. Pang SC, Anderson AM, Chapman TW (2000) J Electrochem Soc 147:444
12. Zhao DD, Bao SJ, Zhao WJ, Hu HL (2007) Electrochem Commun 9:869
13. Cao L, Xu F, Liang YY, Li HL (2004) Adv Mater 16:1853
14. Natile MM, Glisenti A (2003) Chem Mater 15:2502
15. Wang X, Chen XY, Gao LS, Zheng HG, Zhang ZD, Qian YT (2004) J Phys Chem B 108:16401
16. Cao AM, Hu JS, Liang HP (2006) J Phys Chem B 110:15858
17. Barrera E, Viveros T, Montoya A, Ruiz M (1999) J Sol Energy Mater Sol Cells 57:127
18. Feng J, Zeng HC (2003) Chem Mater 15:2829
19. Palmas S, Ferrara F, Vacca A, Mascia M, Polcaro AM (2007) Electrochim Acta 53:1439
20. Zhang XJ, Li QL (2008) Mater Lett 62:988
21. Zhu YJ, Wang WW, Qi RJ, Hu XL (2004) Angew Chem Int Ed Engl 43:1410
22. Yu WY, Tu WX, Liu HF (1999) Langmuir 15:6
23. Zhang XJ, Jiang W, Song D, Liu JX, Li FS (2008) Mater Lett 62:2343
24. Liu YK, Wang GH, Xu CK, Wang WZ (2002) Chem Commun 1486
25. Beach E, Brown S, Shqau K, Mottern M, Warchol Z, Morris P (2008) Mater Lett 62(12–13):1957
26. Dong LH, Chu Y, Liu Y, Li MY, Yang FY, Li LL (2006) J Colloid Interface Sci 301:503
27. Palmas S, Ferrara F, Vacca A, Mascia M, Polcaro AM (2007) Electrochim Acta 53:400